




Research Article

The Potential of Using the Incorporation of Concentrated Solar Power and Gas Turbines in the South of Libya

¹ S. Ehtiwesh , ² A. Gabbasa , ^{3*} I. Ehtiwesh 

^{1,3} Sabratha University, Faculty of Engineering Sabratha, Department of Mechanical Engineering

² University of Zawia, Faculty of Oil & Gas and renewable energy Engineering

E-mail: ^{3*} ismael.ehtiwesh@sabu.edu.ly

Received 10 May 2023, Revised 19 August 2023, Accepted 30 August 2023

Abstract

In the southern part of Libya, there are a number of power plants and other large industrial developments using their power systems, such as petroleum fields. Gas turbines are frequently employed due to water scarcity in the region, such as the Asrir field power plant. However, fuel transportation is one of the main difficulties regarding cost and safety. The annual cost of fuel operation and transportation is admitted to be very high; therefore, this work aims to utilize solar energy potential to reduce fuel consumption. In this context, a power plant that is currently in operation in Libya, which is located close to the Sahara Desert in the southwestern region, was selected as a case study. The region was chosen because it offers extraordinary conditions for the establishment of concentrated power plants. Simulations studies were carried out at full load considering the nature of the solar flux that varies with the meteorological conditions and the thermodynamic calculations were made based on algebraic equations describing the power cycle and the solar field. In addition, the feasibility of fulfilling the power cycle's energy required using the CSPs system was also analyzed. The annual behavior of the solar field was determined using hourly data within the system advisor model (SAM) software. In order to examine the possibility of fuel reduction, the cost of fuel was linked with an exergy analysis from an economic perspective. The findings revealed that the plant efficiency could be increased and the fuel mass rate ratio could be reduced by preheating the air temperature entering the combustion chamber. The air/fuel ratio at the combustor was found 43, the design heat energy required to deliver to the combustion chamber is 414.4MW, and the energetic thermal efficiency of the power cycle is 32.6%. The thermal power design of the solar field is 532MW when average direct irradiation is equal to 1000kWh/m².

Keywords: Concentrated solar power; gas turbine; reduction of fuel consumptions; solar energy.

1. Introduction

The present study aims to address the potential of incorporating concentrated solar power systems (CSPs) as a sustainable alternative to clean energy generation within a gas turbine near a Sahara in Libya. CSPs transform radiant energy into thermal energy, and they cover a large array of different options, the most common ones are: parabolic trough, central receivers (power tower), parabolic dish and linear Fresnel [1]. The central receivers technology is selected due to gas power plants require a high temperature, it uses a large number of mirrors (heliostats) to concentrate the rays on a particular receiver that is placed at the top of a tower [1]. Their operation is expanding, particularly, in the US and Spain [2]; several commercial central receiver plants presently in operation use direct steam generation (DSG) technology; and some use molten salts as both the HTF and storage medium [3]. This technology achieves very high temperatures up to 800°C, thereby increasing the efficiency at which heat is converted into electricity in the power block and reducing the cost of thermal storage. An incorporated solar combined plant is modeled and simulated in the study [4] considering 20% solar, in the east of Algeria, where the region is near the location under study, therefore, the environmental conditions are similar.

The plant uses a gas turbine with exhaust heat recovery for steam generation and the overall efficiency is 49% at a nominal output. Experimental research [5] addressed the effects of forced convective cooling on the electrical and thermal performance of photovoltaic thermal collectors using two different angular-positioned finned heat sink attachments and a phase transition material (paraffin) with steel foam mixture. Air was forced to flow between the flat and angled fins with the use of a fan. Data from a reference photovoltaic module was used to determine solar radiation, temperature, electrical and thermal power, energy, and efficiency efficiencies. In comparison to the solar module, the inclined and flat-finned heat sink attached collectors were cooled by about 12% and 22%, respectively. Due to the given cooling, the electrical efficiency improvement with incline finned and flat finned heat sink application obtained roughly 5% and 6% compared to the solar module, which has a 4.4% electrical efficiency. Overall, the efficiencies were around 60% and 41%. The energy efficiency of photovoltaic modules is 4.7%; cooling with incline finned heat sink and a flat finned heat sink application increases it to 5.6% and 6.9%. Abdel Dayem et al. [6] investigated a numerical analysis considering an integrated solar combined cycle power plant taking in the

Makkah region. The result was compared with the data of the Kuraymat power plant. The capacity of the plant is 135MW, including 61MW that produced within the CSP system. The analysis presents that the model in Makkah is viable and it can be used by the electrical sector in Saudi Arabia. Poullikkas [7] carried out a feasibility analysis aiming to investigate whether the installation of CSPs in the Mediterranean region is economically feasible. The analysis included Cyprus's solar potential as well as all information available regarding the current RES policy of the Cyprus Government, including the applicable feed-in tariff of 0.26 cents per kWh. It is concluded that the implementation of CSPs in the region is profitable and economically feasible under appropriate conditions, namely, the plant size, the storage size, the initial and land cost. Furthermore, the investment can be increasingly attractive by increasing the plant size. The outcomes also showed that the additional benefit resulting from the 30€/t trading price for CO₂ emissions in all situations evaluated throughout the simulations was at 2.4€/kWh. The findings showed that land leasing price has a negative impact on final production costs, increasing the cost of electricity produced by the solar thermal power plant by 1.43€/kWh for every 1€/m² year rise in land leasing price. Studies [1, 8, 9, 10] follow the methodology proposed in [11], which is used to analyze the feasibility of installing CSPs along the Libyan coastline. The potential of solar resources and the appropriate factors for the use of CSPs in Tunisia was evaluated [12], the interconnection of electricity with Europe, and the opportunity for the development of renewable energy sources in North Africa by European support. The study indicates that the electricity generation exceeds the Andasol plant by 1793MWh. Experimental study [13] aimed at the energy and exergy analysis of Al₂O₃ Nano fluid circulation in two different flow patterns was done on PV/T collector cooling. The comparison module was a 20W polycrystalline PV module. The PV/T collectors were also built using the same PV modules. PV/T-A and PV/T-B collectors cooled PV modules by 29% and 48.5% more effectively when subjected to solar radiation of 793 W/m² (equal to 121W of solar power). Environmental economics were predicted to have a size of 0.094tCO₂/year, 0.12tCO₂/year carbon reduction, and corresponding carbon trade values of 1.4 and 1.8 dollars.

Natural gas power plants are available in two technologies, namely, simple cycle and combined cycle gas plants (CCGT) [14]. The integration of CSPs with natural gas plants can be directed to the steam cycle or to gas cycle. Therefore, solar energy produced by CSPs can be used to boil water in the heat recovery steam generator and inject it into the high-pressure turbine or to preheat the air before enters the combustor. The available hybrid-CSPs are mostly integrated with CCGT with the purpose of supplying additional saturated steam to the heat recovery steam generator via a high-pressure drum [3]. The incorporation of CSPs with natural gas can be employed by using several configurations at difference temperatures. Adding heat to gas turbines by CSPs technologies is a technical challenge as gas turbines operate at temperatures higher than steam turbines. On the other hand, the flexible operation of Brayton cycle where the fuel and air can be controlled, makes their combining with CSPs more valuable [15]. Therefore, CSPs adds heat to the power cycle to preheat the air before the combustion chamber, where the fuel rate control assures combustion can get the needed operation

temperature. Furthermore, there is another configuration of integration CSPs with a gas turbine where steam inject (STIG) into the combustor, by replacing or supplementing the steam generators. This technique can increase the generated power and increase the solar share [16, 17], and using this configuration does not need a high temperature from CSP. Moreover, depending on the compression ratio of the gas turbine, STIG can use simple and less expensive CSP technology such as parabolic trough, with saturation steam temperature in a range of 200–300°C. However, the STIG cycle needs water, and the water would be lost if not captured at the turbine exhaust. Solar energy is plentiful in sites where water is scarce and therefore the water consumption of the solar STIG cycle must be addressed. Therefore, preheating the air before in CSP straight to a Brayton cycle, which uses less water, is the proper option [18, 19, 20, 21].

Areas with high sun irradiation levels are most suited for solar thermal power facilities. These characteristics are prevalent in the majority of coastal and southern Saharan regions of Libya, and they are dominated by a large-scale Mediterranean climate with average annual levels of irradiation of (1600–1800kWh/m²) [22], which are quite suitable for practical applications. The Southern region of Libya has a high potential for CSP operation, namely, the Sunbelt region which offers excellent conditions for various commercial applications [8] within a direct normal irradiation (DNI) higher than 2000kWh/m² per year. There are several power plants in the south of Libya and large industrial projects such as petrol fields. Due to the water scarcity in the region, all currently operational power facilities employ gas turbines, such as the one in the Asrir field. However, in terms of cost and safety, fuel transportation is one of the major challenges. In addition to fuel cost, it is acknowledged that the annual cost of fuel transportation is also large; therefore, this work aims to study the incorporation of hybrid solar gas turbine in order to evaluate the potential of reducing the fuel consumptions. A power plant that is currently in operation, which is located close to the Sahara Desert, Ubari power plant was selected as a case study. The region offers outstanding conditions of CSPs rollout, namely: very high DNI, and a large amount of free flat land [23]. The Ubari power plant is located around 700 km from the Zawiya Refinery that feeds it the diesel, where the petroleum brings from the El-Sharara oil field. The Ubari power plant consists of four gas turbine units with a total capacity of 640 megawatts [24], the design power of each unit is 160MW. Figure 1 displays the monthly global horizontal and diffuse radiation for the region under study; the maximum radiation and minimum radiation correspond to July and December, respectively. Figure 2 shows the sunshine duration each month receives, June and July have the highest sunshine period, averaging more than 12 hours per day.

The concept behind the proposed system is to use concentrated solar power technology to harness solar radiation to heat up the air leaving the compressor before it enters the combustion chamber when the weather is sunny. As a result, the air itself is used as the working substance in the receiver instead of another working liquid. The operation temperature of the proposed technology (central receivers) is about 800 degrees Celsius, where the air goes through the tubes inside the receiver that heat up by a field of mirrors, which focus the rays of the Sun onto the receiver.

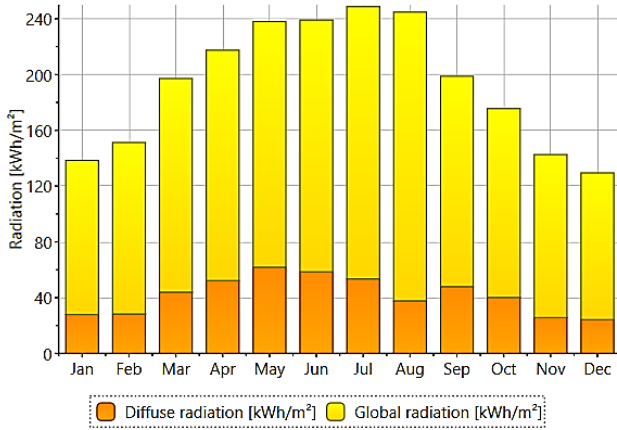


Figure 1. Daily global horizontal irradiation and normal direct irradiation of Ubari [25].

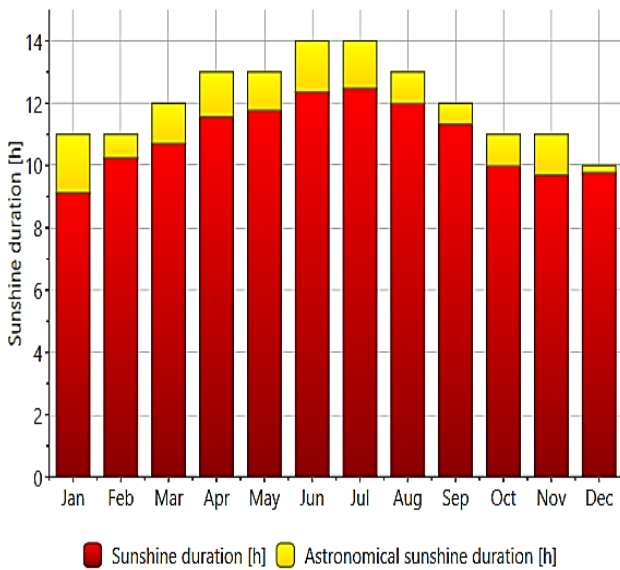


Figure 2. Average daily sunshine duration of Ubari region [25].

The variable nature of the solar flux means that the solar heat input to the gas-turbine is not constant, but varies with current meteorological conditions. In order to maintain a constant temperature at the entrance of the turbine, the fuel-flow to the combustion chamber is continuously controlled. An example of the operation of a hybrid solar gas-turbine is shown in Figure 3. The relative distribution of the heat input to the gas-turbine cycle depends upon the available solar flux. During daytime, heat from the solar sub-system can be harnessed by the gas-turbine, partly (or completely) replacing the heat input from fuel combustion and fuel flow to the combustion chamber decreases below the nominal value. Despite the drop in fuel flow, the combination of solar and fuel heat input provides the required nominal heat input to the gas-turbine, maintaining nominal electricity production. At night-time, the operation of the power plant continues in pure fossil-fuel mode. As such it is important to maintain high overall conversion efficiency for the power plant. If the power block efficiency is low, high carbon emissions during cloud passages and night-time operation can outweigh any savings achieved during solar operation. The present study aims to address the potential of incorporating concentrated solar power systems. The thermodynamic calculations of the selected power cycle were made using algebraic operations; and the feasibility of fulfilling the energy required in the combustion chamber

with the CSPs system was also analyzed. The System Advisor Model environment (SAM) [26], which has an embedded module of the TRNSYS environment, to examine the performance and economic viability of solar units can be utilized solely as a tool to estimate the thermal energy delivered to the solar receiver. However, SAM software is not equipped to handle a gas-cooled solar receiver and the associated power block (i.e., a Brayton Cycle). As such, any economic predictions are invalid, due to the many differences between gas and steam turbines and solar receivers. SAM will be used to calculate the optimal solar field layout, which can then be used to calculate the solar field size, thermal power and air temperature delivered to the power cycle on an hourly basis over the year.

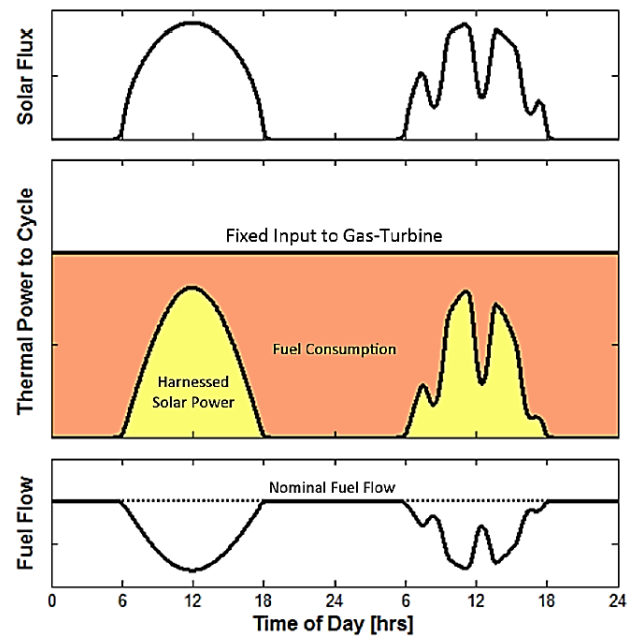


Figure 3. Operation of hybrid solar gas-turbine [27].

2. Mathematical model

For the electricity generation from the concentrated solar power systems, the thermal energy received at the solar field is required to be converted by an appropriate power cycle. The thermodynamic characterization was conducted along with the thermodynamic properties (P , T , v , h , s), which are determined for the operating state points of the cycle based on algebraic equations describing the power cycle and the solar field as depicted in Figure 4.

The ambient atmospheric temperature and pressure used for the compressor inlet are 25°C and 1atm , respectively, and the outlet pressure is calculated based on the design pressure ratio. The exergy balance at each state point is given as follows:

$$\dot{E}_x = \dot{m} * \left[(h_{out} - h_{in}) - T_0 \left(S_{out} - S_{in} - R \ln \left(\frac{P_{out}}{P_{in}} \right) \right) \right] \quad (1)$$

where h is the enthalpy, S is the entropy generation, which measures the irreversibilities generated during a process, \dot{E}_x is the exergy, and \dot{m} is mass flow, except at the chamber combustion, a mixture of air/fuel is considered.

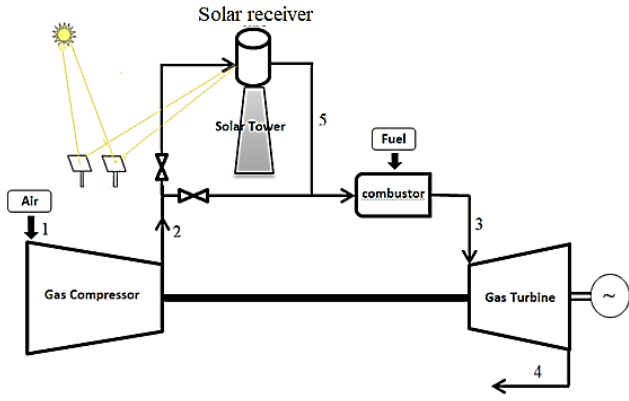


Figure 4. Sub-components of the hybrid solar gas-turbine unit.

It is possible to identify crucial information and understanding of subjects where significant advancements could be made by characterizing the utilization of energy resources in society in terms of exergy by the use of effective technologies, such as more effective energy resource conversions. In principle, the exergy matter can be determined by bringing it to the dead state by means of reversible processes. The thermodynamic analysis of the power cycle uses the net output thermal capacity as the objective function in the optimization process. The components associated with the cycle were analyzed under the assumption of steady-flow. The model is structured to define the properties at each state point of the cycle depicted in Figure 2 and then, sequentially, to determine energy, exergy, efficiency and irreversibility for each power cycle component. The energy and exergy balance are given as follows:

$$T_2 = \left(\frac{P_2}{P_1}\right)^{(k-1)/k} T_1 \quad (2)$$

$$\dot{W}_{comp} = \dot{m}_{air} * (h_1 - h_2) \quad (3)$$

$$\dot{E}_{x,1} = \dot{m}_{air} * \left[(h_1 - h_0) - T_0 \left(S_1 - S_0 - R \ln \left(\frac{P_1}{P_0} \right) \right) \right] \quad (4)$$

$$\dot{E}_{x,2} = \dot{m}_{air} * \left[(h_2 - h_0) - T_0 \left(S_2 - S_0 - R \ln \left(\frac{P_2}{P_0} \right) \right) \right] \quad (5)$$

$$\dot{E}_{xD,comp} = \dot{E}_{x,2} - \dot{E}_{x,1} - \dot{W}_{comp} \quad (6)$$

where \dot{E}_{xD} the exergy destruction.

$$\eta_{II,com} = \frac{\dot{E}_{x,2} - \dot{E}_{x,1}}{|\dot{W}_{comp}|} \quad (7)$$

$$\dot{W}_{Turbine} = \dot{m}_{gas} (h_3 - h_4) \quad (8)$$

$$\dot{E}_{x,3} = \dot{m}_{gas} * \left[(h_3 - h_0) - T_0 \left(S_3 - S_0 - R \ln \left(\frac{P_3}{P_0} \right) \right) \right] \quad (9)$$

$$\dot{E}_{x,4} = \dot{m}_{gas} * \left[(h_4 - h_0) - T_0 \left(S_4 - S_0 - R \ln \left(\frac{P_4}{P_0} \right) \right) \right] \quad (10)$$

$$\dot{E}_{xD,turbine} = \dot{E}_{x,3} - \dot{E}_{x,4} - \dot{W}_{Turbine} \quad (11)$$

$$\eta_{II,Turbine} = \frac{\dot{W}_{Actual,Turbine}}{\dot{E}_{x,3} - \dot{E}_{x,4}} \quad (12)$$

The thermal efficiency gauges the extent to which the energy input to the working fluid passing through the combustor is converted to mechanical output. Its determination is calculated as follows:

$$\dot{W}_{net} = \dot{W}_{Turbine} - \dot{W}_{com} \quad (13)$$

$$\dot{Q}_{in} = \dot{m}_{gas} (h_3 - h_5) \quad (14)$$

$$\eta_{I,Total} = \frac{\dot{W}_{net}}{\dot{Q}_{in}} \quad (15)$$

The quantity of heat gained by the combustion chamber \dot{Q}_{in} may come just from fuel combustion when the sun is not present, or it may come from both the burning of fuel and thermal energy from the solar field when sufficient solar radiation is available. The combustor operates at a steady state steady flow with no heat transfer with the surrounding. The specific exergy of the fuel at environmental conditions reduces to chemical exergy, which can be written as [28, 29]:

$$\varepsilon_{fuel} = \gamma_{fuel} H_{fuel} \quad (16)$$

where ε_{fuel} is the fuel specific exergy, γ_{fuel} the exergy grade function, and H_{fuel} the higher heating value of the fuel. Table 1 reported the higher heating value, chemical exergy, and fuel exergy grade function of different fuels, namely, natural gas and diesel [29].

Table 1. Ratio of fuel chemical exergy to lower heating value.

| Fuel | H_{fuel} (kJ/kg) | ε_{fuel} (kJ/kg) | γ_{fuel} |
|-------------|--------------------|------------------------------|-----------------|
| Diesel | 39500 | 42265 | 1.07 |
| Natural Gas | 55448 | 51702 | 0.93 |

All values of the exergy grade function are close to unity. Consequently, the common practice in such cases is to assume that the exergy of the fuel is approximately equal to the higher heating value [28]. The combustor operates at steady state steady flow with no heat transfer with the surrounding.

$$\dot{E}_{x,fuel} = \dot{m}_{fuel} \varepsilon_{fuel} \quad (17)$$

$$\dot{E}_{xD,combustion} = \dot{E}_{x,fuel} + \dot{E}_{x,2} - \dot{E}_{x,3} \quad (18)$$

$$\eta_{II,Total} = \frac{\dot{W}_{net}}{\dot{E}_{x,fuel} + \dot{E}_{x,5}} \quad (19)$$

The cost rate of exergy destruction of fuel \dot{C}_{fuel} (\$/h) is calculated based on the specific exergetic cost (SPECOC) method, as follows [30]:

$$\dot{C}_{fuel} = c_{fuel} \dot{E}_{x,fuel} \quad (20)$$

where c_{fuel} is the fuel cost rate per unit exergy (\$/kW-h). The objective of the steady-state combustion chamber model is to calculate the nominal mass flow of fuel required to drive the gas-turbine. The composition of the combustor

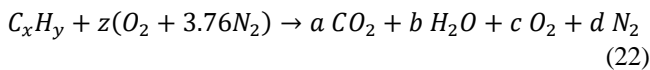
outlet gases must also be determined. The following assumptions have been used for the model of the combustor:

- Complete combustion occurs.
- No thermal losses from the combustion chamber.
- The water content of the combustion air is negligible.

The required mass flow of fuel can be determined by a simple energy balance in the combustion chamber. The energy released during the combustion of the fuel must be sufficient to heat the air by the solar field to reach the desired combustor outlet temperature. The mixture of air and fuel entering the combustor produces gas at a flow rate equal to the sum of the air and fuel, as determined by the following equation, with a fixed nominal pressure drop of 4% [27].

$$\dot{m}_{gas} = \dot{m}_{air} + \dot{m}_{fuel} \quad (21)$$

The combustion reaction with a hydrocarbon fuel and air is modeled using Eq. (22) [31], in which the fuel (typically natural gas) is considered a generic hydrocarbon. The minimum amount of air that supplies sufficient oxygen for the complete combustion of carbon, hydrogen, and any other elements in the fuel, which may oxidize is called theoretical air. When complete combustion is achieved with theoretical air, the products contain no oxygen. The assumption that air is 21% oxygen and 79% nitrogen by volume leads to the conclusion that for each mole of oxygen, $79/21 = 3.76$ moles of nitrogen are involved.



This amount of air is equal to 100% theoretical air ($c=0$) [31], in fact, complete combustion is not likely to be reached unless the amount of air supplied is somewhat bigger than the theoretical amount ($c>1$). With the coefficients to the substances called stoichiometric coefficients, the balance of atoms yields the theoretical air amount. Two important components frequently used to measure the ratio of fuel and air is the air/fuel ratio (AF) or the fuel/air ratio (FA) [32]. These ratios are usually expressed on a mass basis, and which can be on a mole basis. The quantities of fuel and air in a given combustion process are typically determined using these parameters. The amount of air in reaction to the amount of fuel is what is known as the air-fuel ratio.

$$AF_{mass} = \frac{m_{air}}{m_{fuel}} = AF_{mole} \frac{M_{air}}{M_{fuel}} \quad (23)$$

where m denotes mass and M denotes moles.

The total enthalpy and entropy of a product gas mixture at the combustion chamber are expressed as given [31]:

$$h = \sum n_i h_i \quad (24)$$

$$s = \sum n_i s_i - R \sum n_i \ln n_i \quad (25)$$

where n_i = moles of gas i . The model layout is representative of a utility-scale hybrid solar power plant, in which the large size of the power block requires the gas-turbine to remain at the base of the tower. Only radiation

losses are significant at high temperatures was assumed for the model of the solar receiver. The basic energy balance at a solar receiver was taken into consideration the solar heat input to the receiver, the useful thermal power extracted Q_{useful} , and the rate of heat loss. For the receiver energy balance can be expressed using Eq. (26) [27], where $Q_{received}$ is the thermal power collected by the solar receiver.

$$Q_{useful} = Q_{received} - Q_{loss} \quad (26)$$

$$Q_{loss} = A_r \epsilon_r \sigma \left(\left(\frac{T_2 + T_5}{2} \right)^4 - T_o^4 \right) \quad (27)$$

where, Q_{useful} is the thermal power delivering to the power cycle, σ is the Stefan-Boltzmann and $Q_{received}$ can be used to estimate the solar field size using the following equation:

$$Q_{received} = \eta_{opt} \alpha_r DNI . N_h . A_h \quad (28)$$

where A_r is receiver area, A_h is the heliostat area, N_h is the number of heliostats in the field, η_{opt} is the optical efficiency of the receiver, and the absorptivity and emissivity of the volumetric absorber, α_r and ϵ_r respectively. The optical efficiency of the receiver considers the effects of the quartz glass cover that maintains the pressure within the receiver. Higher operating pressures require thicker glass, which reduces the optical efficiency due to higher reflection and absorption at the glass window; this effect is considered in Eq. (29). The reference values for the operating pressure and optical efficiency are presented in [27], their values are 6.5 bar and 87%, respectively.

$$\log(\eta_{opt}) = \frac{P_2}{P_{ref}} \log(\eta_{opt}^{ref}) \quad (29)$$

The pressure losses with the receiver modules are estimated using Eq. (30) based on the mass flux G_r within the receiver, the operating pressure and the mean temperature within the receiver. Reference values are presented in [27], with a reference pressure drop of 40mbar, a reference mass flux G_{ref} of 1.063kg/m²s, and a reference mean temperature of 700°C [27].

$$\frac{\Delta p_{receiver}}{\Delta p_{ref}} = \frac{G_r^{ref} P_{ref}}{G_r P_2} \left(\frac{T_2 + T_5}{2 T_{mean}^{ref}} \right) \quad (30)$$

3. Results

The simulation was carried out at full load and the nominal design conditions are presented in Table 2. The variable nature of the solar flux means that the solar heat input to the gas turbine is not constant, but varies with current meteorological conditions. In order to maintain a constant temperature at the entrance of the turbine, the fuel flow to the combustion chamber is continuously controlled. The relative distribution of the heat input to the gas-turbine cycle depends upon the available solar flux. During the daytime, heat from the solar sub-system can be harnessed by the gas turbine, partly (or completely) replacing the heat input from fuel combustion and fuel flow to the combustion chamber decreases below the nominal value. Despite the drop in fuel flow, the combination of solar and fuel heat input provides the required nominal heat input to the gas turbine, maintaining nominal electricity production. At night-time, the operation of the power plant continues in pure fossil-fuel mode.

Table 2. Nominal design parameters.

| Parameter | Amount |
|----------------------------|-----------------------|
| Design electric power | 160 MW |
| Generator efficiency | 85% |
| Turbine efficiency | 90% |
| Air volume flow rate | 427 m ³ /s |
| The reference state of air | 25°C, 1.013bar |
| Compressor pressure ratio | 10 |

The first simulation was carried out for a sample Brayton cycle without solar integration. Table 3 reports the stream state points' derived thermodynamics characteristics data, where the outcomes of the energetic and exergetic analysis are listed in Table 4, and Table 5 reported the flow rates of air, fuel and gas, which computed at the nominal parameters.

Table 3. Stream data for the power cycle.

| S. ID | state | Temperature (C) | Pressure (kPa) | Enthalpy (kJ/kg) | Entropy (kJ/kg K) |
|-------|----------|-----------------|----------------|------------------|-------------------|
| 1 | Air | 25 | 101.3 | 307.5 | 6.89 |
| 2 | Air | 249.4 | 1013 | 526.5 | 6.768 |
| 3 | Fuel Gas | 1000 | 1013 | 1364 | 6.587 |
| 4 | Gases | 588.9 | 102.8 | 890.8 | 6.796 |

Table 4. Energetics and exergetics of the power cycle components.

| Components | Energetic MW | Exergetic input MW | Exergetic output MW |
|------------|---------------|--------------------|---------------------|
| Compressor | 105.85 (work) | 64.8 | 218.8 |
| Combustion | 414.4 (heat) | 690.2 | 683.7 |
| Turbine | 234.1 (work) | 683.7 | 6.9 |

Table 5. Cycle parameters obtained at nominal conditions.

| Variables | Amount | Units |
|-------------------|--------|-------|
| \dot{W} | 144 | MW |
| \dot{m}_{air} | 483.4 | kg/s |
| \dot{m}_{fuel} | 11.22 | kg/s |
| \dot{m}_{gases} | 494.7 | kg/s |
| η_{cycle} | 32.6 | % |

In conclusion, the average amount of energy needed to be delivered at the combustor is 414.4MW. The fuel mass flow rate is 11.22kg/s, the energetic thermal efficiency of the power cycle is 32.6% and the gross power output is 144MW, respectively. The second part aims to address the analysis of the solar systems; an accurate and comprehensive study of the performance and behavior of solar energy systems and their components; is required to conduct an hourly analysis on an annual basis. The reference of collected thermal power to be delivered by the solar receiver to the power block is considered based on the combustor energy presented in Table 4 (414MW_{th}).

The selection of the design thermal power is depended on two components, namely, optical solar field efficiency and solar multiple. The ratio of the thermal power generated by the solar field at the design point to the thermal power needed by the power cycle under nominal conditions is known as the solar multiple. High SM values without thermal storage function result in thermal energy overproduction that cannot be used to generate electricity. For solar-only systems like the present investigation, the SM is always bigger than one in order to maintain the power cycle's nominal conditions for a longer period of time than would be the case if the solar multiple were equal to one [33]. However, thermal energy overproduction can be useful only if a thermal energy storage system is used, otherwise, like the present study, economically no need to

employ a high value of SM that increases the size of the solar field, which raises costs and necessitates the need for larger land. As the solar multiple increases, the marginal cost of extending nominal receiver operation increases exponentially because the cost of the solar field is generally proportional to the solar multiple. Therefore, the design thermal power calculated for this analysis is 532MW_{th} based on solar multiple equal to 1.28 [33].

Then, SAM is utilized in this study solely as a tool to estimate the thermal power produced by the solar field. SAM can calculate the optimal heliostat field layout, which can then be used to calculate the total power delivered to the solar receiver on an hourly basis for the entire year. Table 6 reported the solar field geometrical and optical parameters and specifications used in the present investigation optimized by SAM environment, where SM, thermal power design and DNI are 1.28, 532MW_{th} and 1000 W/m², respectively. Figures 5 presented the daily average of air temperature collected by the receiver that leaves the solar field to the power cycle for each month. Figure 6 reported daily average of the received thermal power and useful thermal power delivered to the power cycle. The value of zero indicates that gas backup is now being used in place of solar heat flux. These results of the SAM simulation can be extracted into a data file for further calculations and analyses.

It can be noted that the solar share ranges between 6 hours in winter (December) to 12 hours in the summer (June) over the year. The useful thermal power that sends to power cycle varies between around 300MW_t on December and 415MW_t in July. Achieved temperature varies between around 650°C in the winter and 800°C in the summer.

Table 6. Geometrical and optical parameters for the solar field.

| | |
|------------------------------|-----------------------|
| Solar Multiple | 1.28 |
| Design point DNI | 1000 W/m ² |
| Thermal power design | 532 MW _{th} |
| Heliostat width | 12.2 m |
| Heliostat height | 12.2 m |
| Tower height | 187 m |
| Receiver material type | Stainless ASI316 |
| Receiver tube outer diameter | 40 mm |
| Receiver heat loss factor | 1 |

Figure 7 demonstrated the hourly data based on an annual average profile of receiver optical and thermal efficiencies. Thermal efficiency is known as the ratio of received energy to useful energy, and its impact on the outcomes of Figure 6 is evidently proportional. Table 7 reported the first and second efficiencies for the model, fuel mass rate, The cost rate of exergy destruction of fuel, and exergy destruction rate, respectively, variation with the air temperature entering the combustor. As expected, the thermal energy efficiency is increased by raising the temperature of the air before it enters the combustion chamber, and the fuel rate is decreased, therefore, the air mass flow rate entering the combustion is decreased. The exergy destruction rate is decreased with the increase in the air temperature entering the combustor. The fuel cost per unit exergy is selected based on the Baghernejad et al. study [30], 0.012\$/MJ-h; the fuel cost rate decreased with the increase in the air temperature entering the combustion chamber.

For the solar sole scenario (no combustion), the range of the prediction air temperature produced by the solar system

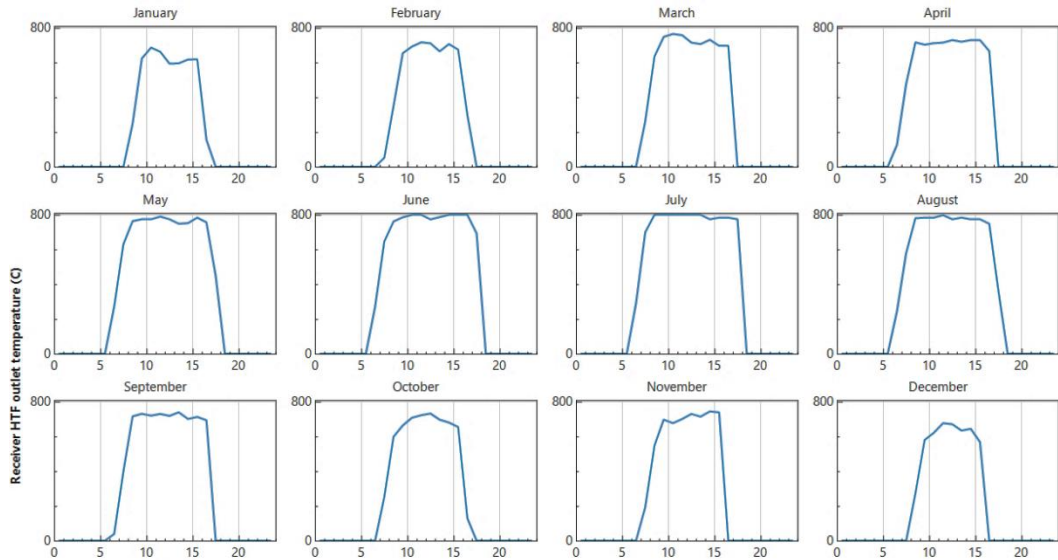


Figure 5. Solar field outlet temperature.

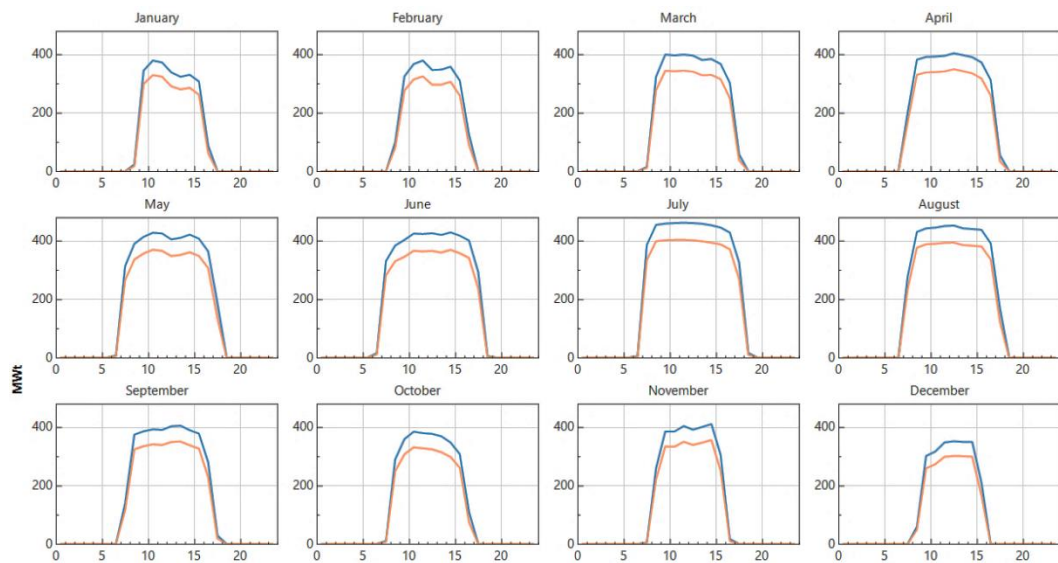


Figure 6. Solar field received (Blue) and useful thermal power (Orange).

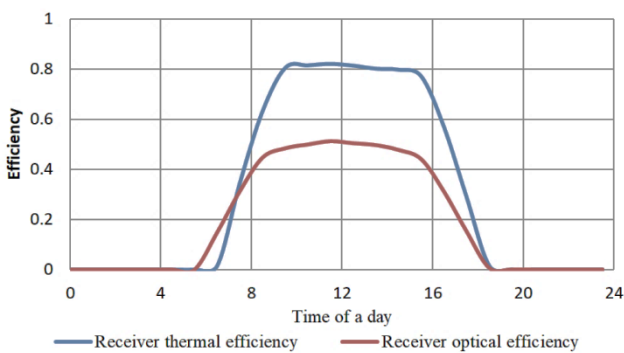


Figure 7. Annual average profile of the solar receiver's optical efficiency.

that enters the turbine is depending on the available solar flux, in particular produced air temperature. To generate 144MW (Design) at 750°C, the air flow rate is found equal to 430 kg/s. Therefore, for the solar sole scenario at varying air temperature that delivered by the solar field directly to the turbine, Figure 8 shows how the power cycle electricity output varies with air temperature inlet the turbine at different flow rates. The equilibrium between the air flow rate and solar heat flux is crucial for maintaining the air at

the highest temperature. It can be noted that when the air temperature produced by solar field is high (750°C) (solar only case study), the air mass flow (≈ 430 kg/s) is less than the design flow rate.

Table 7. Combustion temperature inlet variation with various results.

| $T_{\text{comb, inlet}}$ °C | \dot{C}_{fuel} \$/h | $\dot{E}_{x, \text{comb}}$ MW | \dot{m}_{air} kg/s | \dot{m}_{Fuel} kg/s | η_I | η_{II} |
|--------------------------------|---------------------------------|----------------------------------|--------------------------------|---------------------------------|----------|-------------|
| 250 | 20350 | 20.35 | 482 | 11.2 | 0.326 | 0.301 |
| 300 | 19082 | 19.08 | 452 | 10.5 | 0.334 | 0.308 |
| 350 | 17801 | 17.80 | 421 | 9.81 | 0.344 | 0.316 |
| 400 | 16506 | 16.51 | 391 | 9.10 | 0.354 | 0.325 |
| 450 | 15197 | 15.19 | 360 | 8.37 | 0.367 | 0.336 |
| 500 | 13874 | 13.87 | 328 | 7.64 | 0.382 | 0.349 |
| 550 | 12537 | 12.54 | 297 | 6.91 | 0.401 | 0.366 |
| 600 | 11186 | 11.19 | 265 | 6.16 | 0.424 | 0.387 |
| 650 | 9823 | 9.82 | 232 | 5.41 | 0.454 | 0.413 |
| 700 | 8447 | 6.17 | 200 | 4.65 | 0.494 | 0.449 |
| 750 | 7059 | 6.15 | 167 | 3.89 | 0.549 | 0.498 |

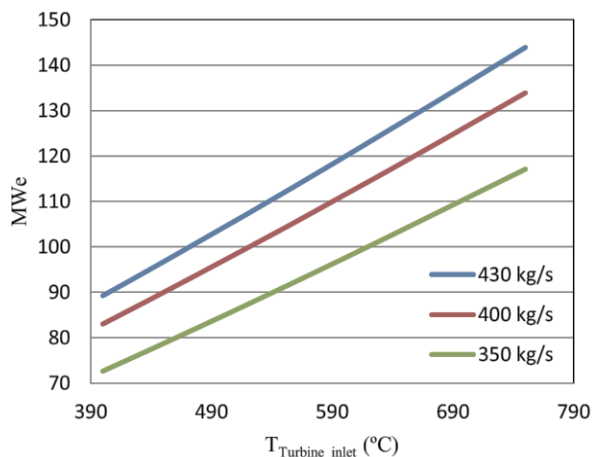


Figure 8. Variation in electricity production with turbine inlet air temperature for various air flows.

4. Conclusion

The potential of incorporating concentrated solar power systems with gas turbine was investigated considering the Ubari power plant. The main objective is to reduce the high operating and transportation costs for petroleum in the southern part of Libya, and therefore, to reduce the environmental harm that fuel causes. Analysis of the straightforward Brayton power cycle without solar function was carried out, and the conclusions were used as a design guide for the design and analysis of the solar field. The simulation was carried out at full load; the variable nature of the solar flux means that the solar heat energy delivered to the power cycle is not constant, and varies with current meteorological conditions. In order to maintain a constant temperature at the turbine inlet, the fuel flow to the combustion chamber is continuously controlled. The combustor heat energy required is 414.4MW and the air/fuel ratio is 43; the energetic thermal efficiency of the power cycle is 32.6% and the gross power output is 144MW. An hourly analysis based on an annual basis was simulated within the SAM environment. However, SAM software is not equipped to handle a gas-cooled solar receiver and the associated power cycle, therefore, SAM is utilized in this study solely as a tool to estimate the thermal energy collected by the solar receiver and the actual energy delivered to the power cycle. The designed system can deliver the required energy in about 6 hours in winter (December) and 12 hours in the summer (June). The fuel flow rate and fuel cost associated with exergy destruction are used to assess the economic approach. The analysis presented that by increasing the combustor inlet air temperature, the power cycle efficiency is increased and the fuel mass rate is decreased. The fuel cost rate can be minimized by increase combustor inlet air temperature. The use of sole solar energy requires a big storage system and a huge land, and it does not fulfill its goal during the winter. Therefore, the use of a hybrid solar gas turbine design to use less gas might be the most effective and cost-effective solution; where employing sole gas turbines requires the use and transportation of fuel, which is expensive and harmful to the environment.

Nomenclatures

A Area
 c The cost rate per unit exergy
 \dot{C} The cost rate of exergy destruction
 DNI Direct normal irradiation

\dot{E}_x Exergy
 \dot{E}_{xD} Exergy destruction
 G Mass flux
 h Enthalpy
 H The higher heating
 i Gas type
 M Moles
 m Mass
 \dot{m} Mass flow rate
 n Moles of gas
 N_h Number of Heliostats
 P Pressure
 Q Thermal energy
 s Entropy
 S Entropy generation
 T Temperature
 W Work

Greek symbols

α Absorptivity
 η Efficiency
 ε Emissivity
 ε The fuel specific exergy
 γ The exergy grade function
 σ The Stefan-Boltzmann

Abbreviations

h Heliostats
 o Atmosphere
 opt Optical
 r Receiver
 ref Reference
 SM Solar multiple

References:

- [1] I. A. S. Ehtiwesh, F. Neto Da Silva, and A. C. M. Sousa, "Deployment of parabolic trough concentrated solar power plants in North Africa – a case study for Libya," *Int. J. Green Energy*, Oct. 2018, doi:10.1080/15435075.2018.1533474.
- [2] I. A. S. Ehtiwesh, M. C. Coelho, and A. C. M. Sousa, "Exergetic and environmental life cycle assessment analysis of concentrated solar power plants," *Renew. Sustain. Energy Rev.*, vol. 56, pp. 145–155, 2016, doi:10.1016/j.rser.2015.11.066.
- [3] M. Muñoz and J. Muñoz-ant, "Comparison of Different Technologies for Integrated Solar Combined Cycles: Analysis of Concentrating Technology and Solar Integration," *MDPI, Energies*, 2018, doi:10.3390/en11051064.
- [4] H. Derbal, S. Bouaichaoui, N. El-Gharbi, M. Belhamei, and A. Benzaoui, "Modeling and numerical simulation of an integrated solar combined cycle system in Algeria," *Procedia Eng.*, vol. 33, pp. 199–208, Jan. 2012, doi.org/10.1016/j.proeng.2012.01.1194.
- [5] A. Al Hariri, S. Selimli, and H. Dumrul, "Effectiveness of heat sink fin position on photovoltaic thermal collector cooling supported by paraffin and steel foam: An experimental study," *Appl. Therm. Eng.*, vol. 213, no. June, p. 118784, 2022, doi:10.1016/j.applthermaleng.2022.118784.
- [6] A. Abdel Dayem, M. Metwally, A. Alghamdi, and E.

- Marzouk, "Numerical simulation and experimental validation of integrated solar combined power plant," *Energy Procedia*, vol. 50, pp. 290–305, 2014, doi.org/10.1016/j.egypro.2014.06.036.
- [7] A. Poullikkas, "Economic analysis of power generation from parabolic trough solar thermal plants for the Mediterranean region - A case study for the island of Cyprus," *Renew. Sustain. Energy Rev.*, vol. 13, no. 9, pp. 2474–2484, Dec. 2009, doi.org/10.1016/j.rser.2009.03.014.
- [8] M. Mashena and N. Alkishriwi, "Concentrated Solar Power Potential in Libya," *JASE*, vol. 11, no. 1, pp. 56–72, 2017.
- [9] B. Belgasim, Y. Aldali, M. J. R. Abdunnabi, G. Hashem, and K. Hossin, "The potential of concentrating solar power (CSP) for electricity generation in Libya," *Renew. Sustain. Energy Rev.*, vol. 90, no. March, pp. 1–15, 2018, doi:10.1016/j.rser.2018.03.045.
- [10] T. E. Boukelia, M. S. Mecibah, B. N. Kumar, and K. S. Reddy, "Optimization, selection and feasibility study of solar parabolic trough power plants for Algerian conditions," *Energy Convers. Manag.*, vol. 101, pp. 450–459, 2015, doi:10.1016/j.enconman.2015.05.067.
- [11] I. Ehtiwesh, F. Neto da Silva, and A. Sousa, "Performance and economic analysis of concentrated solar power plants in Libya," in *2nd International Conference on Energy and Environment: bringing together Engineering and Economics*, 2015, pp. 459–66.
- [12] M. Balghouthi, S. E. Trabelsi, M. Ben Amara, A. B. H. Ali, and A. Guizani, "Potential of concentrating solar power (CSP) technology in Tunisia and the possibility of interconnection with Europe," *Renew. Sustain. Energy Rev.*, vol. 56, pp. 1227–1248, 2016, doi:10.1016/j.rser.2015.12.052.
- [13] O. M. J. Jasim, S. Selimli, H. Dumrul, and S. Yilmaz, "Closed-loop aluminium oxide nanofluid cooled photovoltaic thermal collector energy and exergy analysis, an experimental study," *J. Energy Storage*, vol. 50, no. April, pp. 1–9, 2022, doi:10.1016/j.est.2022.104654
- [14] B. A. A. Yousef *et al.*, "Perspective on integration of concentrated solar power plants," no. April, pp. 1098–1125, 2021.
- [15] K. Kitzmiller, "Effect of Variable Guide Vanes and Natural Gas Hybridization for Accommodating Fluctuations in Solar Input to a Gas Turbine," vol. 134, no. November 2012, pp. 1–12, 2016, doi:10.1115/1.4006894.
- [16] M. Livshits and A. Kribus, "Solar hybrid steam injection gas turbine (STIG) cycle," *Sol. Energy*, vol. 86, no. 1, pp. 190–199, 2012, doi:10.1016/j.solener.2011.09.020.
- [17] G. Polonsky and A. Kribus, "Performance of the solar hybrid STIG cycle with latent heat storage," *Appl. Energy*, vol. 155, pp. 791–803, 2015, doi:10.1016/j.apenergy.2015.06.067.
- [18] F. Moreno-gamboa, A. Escudero-atehortua, and C. Nieto-londoño, "Performance evaluation of external fired hybrid solar gas-turbine power plant in Colombia using energy and exergy methods," *Therm. Sci. Eng. Prog.*, vol. 20, no. August, 2020, doi:10.1016/j.tsep.2020.100679.
- [19] K. Mohammadi, K. Ellingwood, and K. Powell, "Novel hybrid solar tower-gas turbine combined power cycles using supercritical carbon dioxide bottoming cycles," *Appl. Therm. Eng.*, p. 1-48, 2020, doi:10.1016/j.applthermaleng.2020.115588.
- [20] P. Schwarzbo, R. Buck, C. Sugarmen, A. Ring, P. Altwegg, and J. Enrile, "Solar gas turbine systems : Design , cost and perspectives," vol. 80, pp. 1231–1240, 2006, doi:10.1016/j.solener.2005.09.007.
- [21] B. Ssebabi, F. Dinter, J. Van Der Spuy, and M. Schatz, "Predicting the performance of a micro gas turbine under solar-hybrid operation," *Energy*, vol. 177, pp. 121–135, 2019, doi:10.1016/j.energy.2019.04.064
- [22] U. Desideri, F. Zepparelli, V. Morettini, and E. Garroni, "Comparative analysis of concentrating solar power and photovoltaic technologies: Technical and environmental evaluations," *Appl. Energy*, vol. 102, pp. 765–784, 2013, doi.org/10.1016/j.apenergy.2012.08.033
- [23] I. Ehtiwesh, "Exergetic , energetic , economic and environmental evaluation of concentrated solar power plants in Libya," PhD thesis, University of Aveiro, 2016, doi:http://ria.ua.pt/handle/10773/15882.
- [24] "GECOL to resume work at Ubari power plant project | The Libya Observer." [Online]. Available: <https://www.libyaobserver.ly/inbrief/gecol-resume-work-ubari-power-plant-project>.
- [25] M. Genossenschaft, "Meteonorm7 Software," *METEOTEST Genossenschaft*, <https://meteonorm.com>
- [26] National Renewable Energy Laboratory (NREL), "System Advisor Model (SAM 2022.12.2 r3 (SSC 280))." <https://sam.nrel.gov/download>.
- [27] J. Spelling, "Hybrid Solar Gas-Turbine Power Plants, A Thermo-economic Analysis," KTH Royal Institute of Technology - School of Industrial Engineering and Management, Doctoral Thesis, 2013.
- [28] I. Dincer, "Renewable energy and sustainable development: a crucial review," *Renew. Sustain. Energy Rev.*, vol. 4, no. 2, pp. 157–175, 2000.
- [29] A. Al-Ghandoor, I. Al-Hinti, B. Akash, and E. Abu-Nada, "Analysis of energy and exergy use in the Jordanian urban residential sector," *Int. J. Exergy*, vol. 5, no. 4, pp. 413–428, 2008, doi:10.1504/IJEX.2008.019113.
- [30] A. Baghernejad and A. Anvari-moghaddam, "Exergoeconomic and environmental analysis and multi-objective optimization of a new regenerative gas turbine combined cycle," *Appl. Sci.*, vol. 11, no. 23, 2021, doi:10.3390/app112311554.
- [31] M. Moran, H. Shapiro, D. Boettner, and M. Bailey, *Fundamentals of engineering thermodynamics*, Seven Edit. John Wiley & Sons, Inc., 2011.
- [32] C. Borgnakke and R. Sonntag, *Fundamentals of Thermodynamics*, Seventh. John Wiley & Sons, Inc., 2009.

[33] M. Montes, A. Abánades, J. Martínez-Val, and M. Valdés, “Solar multiple optimization for a solar-only thermal power plant, using oil as heat transfer fluid in

the parabolic trough collectors,” *Sol. Energy*, vol. 83, no. 12, pp. 2165–2176, Dec. 2009, doi.org/10.1016/j.solener.2009.08.010